Applied Surface Science 423 (2017) 557–565

Contents lists available at ScienceDirect

Applied Surface Science

journal homepage: www.elsevier.com/locate/apsusc

Full Length Article

Osteoconductive properties of two different bioactive glass forms (powder and fiber) combined with collagen

Angela Maria Paiva Magri[a,1], Kelly Rossetti Fernandes[a,1], Fabio Roberto Ueno[a], Hueliton Wilian Kido[a], Antonio Carlos da Silva[b], Francisco José Correa Braga[b], Renata Neves Granito[a], Paulo Roberto Gabbai-Armelin[a], Ana Claudia Muniz Rennó[a,*]

[a] Department of Biosciences, Federal University of São Paulo (UNIFESP), Rua Silva Jardim, 136, Santos, SP, 11015020, Brazil
[b] Nuclear and Energy Research Institute (IPEN), University of São Paulo (USP), Avenida Lineu Prestes, 2242, São Paulo, SP, 05508000, Brazil

ARTICLE INFO

Article history:
Received 25 April 2017
Accepted 14 June 2017
Available online 19 June 2017

Keywords:
Bioactive glasses
Collagen
Composite
Fibers
Powder
Bone repair

ABSTRACT

Bioactive Glasses (BG) is a group of synthetic silica-based materials with the unique ability to bond to living bone and can be used in bone repair. Although the osteogenic potential of BG, this material may have not present sufficient osteoconductive and osteoinductive properties to allow bone regeneration, especially in compromised situations. In order to overcome this limitation, it was proposed the combination the BG in two forms (powder and fiber) combined with collagen type I (COL-1). The aim of this study was to evaluate the BG/COL-based materials in terms of morphological characteristics, physicochemical features and mineralization. Additionally, the second objective was to investigate and compare the osteoconductive properties of two different bioactive glass forms (powder and fiber) enriched or not with collagen using a tibial bone defect model in rats. For this, four different formulations (BG powder – BGp, BG powder enriched with collagen – BGp/Col, BG fibers – BGf and BGp fibers enriched with collagen – BGf/Col) were developed. The physicochemical and morphological modifications were analyzed by SEM, FTIR, calcium assay and pH measurement. For *in vivo* evaluations, histopathology, morphometrical and immunohistochemistry were performed in a tibial defect in rats. The FTIR analysis indicated that BGp and BGf maintained the characteristic peaks for this class of material. Furthermore, the calcium assay showed an increased Ca uptake in the BG fibers. The pH measurements revealed that BGp (with or without collagen) presented higher pH values compared to BGf. In addition, the histological analysis demonstrated no inflammation for all groups at the site of the injury, besides a faster material degradation and higher bone ingrowth for groups with collagen. The immunohistochemistry analysis demonstrated Runx-2 and Rank-L expression for all the groups. Those findings support that BGp with collagen can be a promising alternative for treating fracture of difficult consolidation.

1. Introduction

A series of different artificial materials have been developed to be used as bone graft substitutes [1]. Among those, Bioactive Glasses (BG) comprise a group of synthetic silica-based materials with the unique ability to bond to living bone by forming a biologically active bone-like apatite layer on their surface [2–5]. The original BG, named Bioglass® 45S5, is a melt-derived glass with four components (46.1% SiO_2, 24.4% Na_2O, 26.9% CaO and 2.6% P_2O_5, in mol) and it is known as one of the most bioactive bone-bonding glasses. It has been used in many clinical procedures, including the repair of periodontal bone defects, maxillofacial defects reconstruction, spinal surgery and bone replacement [6,7]. Although the osteogenic potential of BG, this material may have not present sufficient osteoconductive and osteoinductive properties to allow bone regeneration, especially in compromised situations such as osteoporosis or fractures of great extension [8].

In order to overcome these limitations, many composite grafts have been developed trying to associate different characteristics from distinguished materials toward approximating the bone-forming components, providing a better environment for bone formation [9,10]. In this context, some researchers have been combining collagen to bioceramics and bioactive glasses with the intention of mimicking the organic and inorganic part of the bone tissue [11,12]. It is well known that collagen, mainly type I (COL-1),

* Corresponding author.
E-mail address: acmr_ft@yahoo.com.br (A.C.M. Rennó).
[1] Equally contributed.

http://dx.doi.org/10.1016/j.apsusc.2017.06.152
0169-4332/

is the major organic component in the extracellular matrix (ECM) and this protein level is critical for mechanical and biological roles [13].

Besides the composition, another essential point for the graft success is the material structure [13]. In bone tissue engineering, BG have been used mainly in powder, blocks and scaffolds [14,15]. Although, in most cases these biomaterials serve as support of tissue formation, being able of stimulating cell adhesion and angiogenesis, they do not have the ability of acting as fillers for bone defects with irregular shapes [16]. In this context, the moldability found in fibrous materials is a desired characteristic necessary for grafts, allowing to fit irregularly shaped bone defects [17,18]. Additionally, fibrous materials are capable of supporting cell attachment, mineralization and new bone formation in the site of the defect [19,20].

Therefore, the obtainment of malleable fibers from bioactive glasses enriched with collagen seems to be a promising therapeutic approach targeting bone repair. Toward this goal, a fibrous glassy material, with four components (46.1% SiO_2, 24.4% Na_2O, 26.9% CaO and 2.6% P_2O_5, in mol) [7], have been recently developed [21]. In addition, the bioactive material was enriched with type-1 collagen in order to introduce an organic part to the ceramic.

Since there is a growing interest in the development of biomaterials with improved osteogenic properties, it was hypothesized that the introduction of collagen to BG would improve the *in vivo* bioactive properties of the material, providing a bone graft with additional advantages for clinical use. Furthermore, the hypothesis that the fibrous glassy material would present a more adequate morphology, facilitating cell migration and vascularization, was raised. Consequently, the aims of the present study were systematized into 2 points: first, to evaluate the BG/COL-based materials in terms of morphological characteristics, physicochemical features and mineralization. Second, to investigate and compare the osteoconductive properties of two different bioactive glass forms (powder and fiber) enriched or not with collagen using a tibial bone defect model in rats. To this end, samples in 4 different compositions (BG powder: BGp; BG powder enriched with collagen: BGp/COL; BG fibers: BGf; and BG fibers enriched with collagen: BGf/COL) were analyzed by scanning electron microscopy (SEM), x-ray diffraction (XRD), calcium deposition and pH. Also, the biomaterials were implanted into non-critical tibial defects in rats. Histopathological, histomorphometry and immunohistochemistry analyzes were evaluated after 15 days of implantation.

2. Materials and methods

2.1. Materials

2.1.1. BG powder

For the obtainment of BG powder, mineral silica 98.0 wt% powder was purified by attack with hot hydrochloric acid (Merck, P.A.) followed by filtration (fast paper filtration Whatmman 40) and held 30 washings with boiling distilled water for elimination of impurities (R_2O_3) and analyzed by XRF to ensure 99.5 wt% purity. Additionally, the following reagent analytical-grade as sodium hydroxide (NaOH 97.0 wt%, heavy metals ≤ 0.003 wt%, Cl- ≤ 0.005 wt%, Fe ≤ 0.001 wt%, Hg ≤ 0.1 ppm, K ≤ 0.02%, Na2CO3 ≤ 1.0 wt%, NH4OH ≤ 0.02 wt%, Ni ≤ 0.001 wt%, PO43- ≤ 0.001 wt%, SO42- ≤ 0.003 wt%, absorbed water ≤ 2.0 wt%; Nuclear, São Paulo, Brazil), Calcium oxide (CaO 97.0 wt%, heavy metals ≤ 0.005 wt%, Cl- ≤ 0.05 wt%, SO42- ≤ 0.5 wt%, Fe ≤ 0.5 wt%, insolubles ≤ 0.01 wt%, absorbed water ≤ 2.0 wt%; Química Moderna, São Paulo, Brazil), Sodium Phosphate (Na_3PO_4 99.0 wt%, heavy metals ≤ 5 ppm, insolubles ≤ 0.01 wt%, SiO_4 0.005 wt%, PO_4^{3-} ≤ 0.001 wt%, Fe ≤ 5 ppm, Na_2CO_3 ≤ 0.02 wt%, NH_4OH ≤ 0.01 wt%, Ca and Mg ≤ 0.01 wt%, SO_4^{2-} ≤ 0.004 wt%, Cl- ≤ 0.1 ppm; Química Moderna, São Paulo, Brazil) were also used. The chemicals were weighed and mixed for 30 min in a polyethylene bottle. Premixed batches were melted in an alumina crucible at a temperature of 1500 °C (Lindberg Blue vertical super kanthal furnace – USA). The melting time was fixed as 2 h. Samples were quenched in deionized water and milled to powder grain (with sizes ranging from 260 to 600 μm). No annealing was performated.

2.1.2. BG fibers

BG fibers were obtained using the same process described above. However, in spite of quenching in water, the melt was quenched in a Hager-Rosengarth apparatus [21,22]. The Hager-Rosengarth process leads the melt to a centrifugal acceleration, leaving the centrifuging disc and cooled in air which is flowing together with the fiber due to this angle speed [23].

2.1.3. Collagen

Collagen type I used in this study was provided by Consulmat (São Carlos, Brazil). Type I collagen from bovine bone was obtained in three main steps: (i) demineralization of bovine cortical bone in chloridric acid (HCl); (ii) dissolution of the cortical bone collagen in 0.5 M acetic acid ($C_2H_4O_2$) at 40 °C and (iii) pH adjustment with ammonium hydroxide (NH_4OH). Granules <270 μm were obtained.

2.2. Composite preparation

2.2.1. Enrichment of BG powder with COL

Layers of COL and BG powder were alternately deposited on a substrate (Petri dish) insomuch that the resulting particles were completely coated by COL. Samples were dried during 48 h in an oven at 40 °C and the composite was milled to obtain powder.

2.2.2. Enrichment of BG fibers with COL

For the fibrous composition enriched with COL, the collagen solution was homogeneously sprayed on the fibers tappet until it had acquired the wet appearance. Subsequently, the material was dried for 48 h at 40 °C.

2.2.3. Material sterilization

Before use, the materials were sterilized using a 25 kGy dose of gamma irradiation (IPEN, São Paulo, Brazil).

2.3. Characterization of the materials

2.3.1. Morphological characteristics

The morphology of the different materials was first examined by SEM observation (Phenom™, FEI Co.). The composites were mounted on aluminum stubs using carbon tape and sputter-coated with gold/palladium prior to examination.

2.3.2. Fourier transform infrared spectroscopy (FTIR)

FTIR (Thermo Nicolet Nexus 4000, USA) was performed to evaluate the chemical bonds present in the materials. The examinations were done in the range of 400–1800 cm^{-1} with a resolution of 2 cm^{-1}. The samples were scanned 128 times for each measurement and the spectrum acquired was the average of all these scans.

2.3.3. Calcium assay

The Ca release/uptake capacity of the bioactive materials, BGp and BGf, was evaluated according to Kokubo and Takadama [24]. Samples (0.05 g) were placed in glass vials containing 3 mL of Simulated Body Fluid (SBF) at 37 °C on a shaker table (70 Hz) for up to 5 days, with refreshment on days 1, 3 and 5. Subsequently to each refreshment, the solution of the previous period was saved for analysis of the calcium content in SBF by the orthocresolphtalein

complexone (OCPC) assay [25]. These solutions were incubated overnight in 1 mL of 0.5 N acetic acid on a shaker table. For analysis, 300 μL working reagent was added to 10 μL sample or standard in a 96-well plate. Thereafter, the well plate was incubated for 10 min at room temperature. The absorbance was measured on a microplate spectrophotometer at 570 nm (Molecular Device, SpectraMax M5, Sunnyvale, CA, USA). The standards (between 0 and 100 $\mu g\,mL^{-1}$) were prepared using a $CaCl_2$ stock solution. Data were acquired from triplicate samples and measured in duplo. The Ca depletion was plotted cumulatively, measuring the difference between the Ca concentration in the sample-free SBF control solutions and the SBF solution in the presence of the different bioactive glass forms.

2.3.4. pH measurements

After each experimental period, the pH of the SBF solutions in contact with the materials was measured (n = 3) utilizing a pH electrode (Tecnal T.E.C-51, Piracicaba, Brazil).

2.4. In vivo studies

2.4.1. Experimental design and surgical procedure

Forty young adult male Wistar rats (12 weeks old; weight 295 ± 29 g) were used as experimental animals and randomly distributed into the following groups (n = 10): BGp (BG powder); BGp/COL (BG powder enriched with collagen); BGf (BG fibers) and BGf/COL (BG fibers enriched with collagen).

The animal experimental plan was reviewed and approved by the Experimental Animal Committee of the Federal University of Sao Paulo (CEUA N° 4891060616) and national guidelines for the care and use of laboratory animals were observed. Anesthesia was induced and maintained by Isoflurane inhalation (Rhodia Organique Fine Limited). In order to minimize post-operative discomfort, buprenorfine (Temgesic; Reckitt Benckiser Health Care Limited, Schering-Plough, Hoddesdon, UK) was administered intraperitoneally (0.02 mg/kg) directly after the operation and subcutaneously for 2 days after surgery.

For inserting implants into the tibial defects, the animals were immobilized on their back and both hind limbs were shaved, washed and disinfected with povidone-iodine. After exposure of the medial compartment of the tibia, a 1.0 mm pilot hole was drilled. The hole was gradually widened until a final defect size of 3 mm in width was reached. Low rotational drill speeds (max. 450 rpm) and constant physiologic saline irrigation was used. After preparation, the defects were thoroughly irrigated and packed with sterile cotton gaze to stop bleeding. Surgery was performed in both legs of the rats and one defect was created in each tibia. The sterilized compositions were placed in the created defect up to its complete filling (n = 10 per experimental group). Thereafter, the wound was closed with resorbable Vicryl® 5-0 (Johnson & Johnson, St.Stevens-Woluwe, Belgium) after which the skin was closed by staples (Agraven®; InstruVet BV, Cuijk, The Netherlands). After 2 weeks of implantation, rats were sacrificed by CO_2 asphyxia. The tibias were collected for analysis.

2.4.2. Histological procedures

For the histopathological, morphometrical and imunohistochemical analysis, the tibiae were harvested and fixed in 10% buffer formalin (Merck, Darmstadt, Germany) for 24 h. They were decalcified in 10% EDTA (Merck) and embedded in paraffin blocks. Five-micrometer cortical bone slices were obtained with a microtome (Leica Microsystems SP 1600, Nussloch, Germany). The slices were cut perpendicularly to the medial-lateral drilling axis of the implant. At least three non-consecutive sections of each specimen were stained with hematoxylin and eosin (H.E stain, Merck) and used for analysis.

2.4.3. Histopathological analysis

Histopathological evaluation was performed under an optical microscope (Olympus, Optical Co. Ltd, Tokyo, Japan). The area of the bone defect was qualitatively evaluated considering the inflammatory process, granulation tissue and newly formed bone. At least three sections of each specimen were examined for each specimen.

2.4.4. Histomorphometric analysis

For histomorphometric analysis was used a Zeiss microscope (Carl Zeiss Vision GmbH, Germany) and the semiautomatic image-analyzing computer program Osteomeasure (Osteometrics, Inc., Atlanta, Georgia). The percent bone volume (BV/TV) was performed according percentage of area within region of interest (ROI) occupied by bone (magnification of 40×).

2.4.5. Immunohistochemistry analysis

For the immunohistochemical analysis, xylene was used to remove the paraffin from the serial sections. After this procedure, the sections were rehydrated in graded ethanol and pretreated in a microwave (Electrolux, São Paulo, Brazil) with 0.01 M citric acid buffer (pH 6) for three cycles of 5 min each at 850 W for antigen retrieval. The resulting material was pre-incubated with 0.3% hydrogen peroxide in phosphate-buffered saline (PBS) solution for 5 min in order to inactivate the endogenous peroxidase. Then, the samples were blocked with 5% normal goat serum in PBS for 10 min. The specimens were incubated with anti-RUNX-2 polyclonal primary antibody (code: sc-8566, Santa Cruz Biotechnology, USA) at a concentration of 1:200, and anti-RANK-L polyclonal primary antibody (code: sc-7627, Santa Cruz Biotechnology, USA) also at a concentration of 1:200. Incubation was carried out overnight at 4 °C in a refrigerator. This step was followed by two washes in PBS for 10 min. The sections were then incubated with biotin conjugated secondary antibody anti-rabbit IgG (Vector Laboratories, Burlingame, CA, USA) at a concentration of 1:200 in PBS for 1 h. The sections were washed twice with PBS followed by the application of preformed avidin biotin complex conjugated to peroxidase (Vector Laboratories) for 45 min. The bound complexes were visualized by the application of a 0.05% solution of 3-3′-diaminobenzidine solution and counterstained with Harris hematoxylin (Sigma-Aldrich). For control studies of the antibodies, the serial sections were treated with rabbit IgG (Vector Laboratories) at a concentration of 1:200 in place of the primary antibody. Additionally, internal positive controls were performed with each staining bath. RUNX-2 and RANK-L immunoexpression were evaluated qualitatively in order to assess the presence (or absence) and region of occurrence of the immunomarkers. Three sections of each specimen were examined with a light microscopy (Leica Microsystems AG, Wetzlar, Germany).

2.4.6. Statistical analysis

Data were expressed as mean and standard error (SE) of the mean values for each sample. Statistical analyses of the data were executed using SPSS, version 16.0 (SPSS Inc., Chicago, IL, USA). The statistical comparisons were performed using one-way analysis of variance (ANOVA) with Tukey multiple comparison post-test. Differences were considered significant at $p < 0.05$.

3. Results

3.1. Characterization of the materials

3.1.1. Morphological characteristics

SEM evaluations of the different materials are depicted in Fig. 1. As expected, BG particles with diverse sizes could be observed (Fig. 1A and B). The bioactive glass particles within BGp/COL

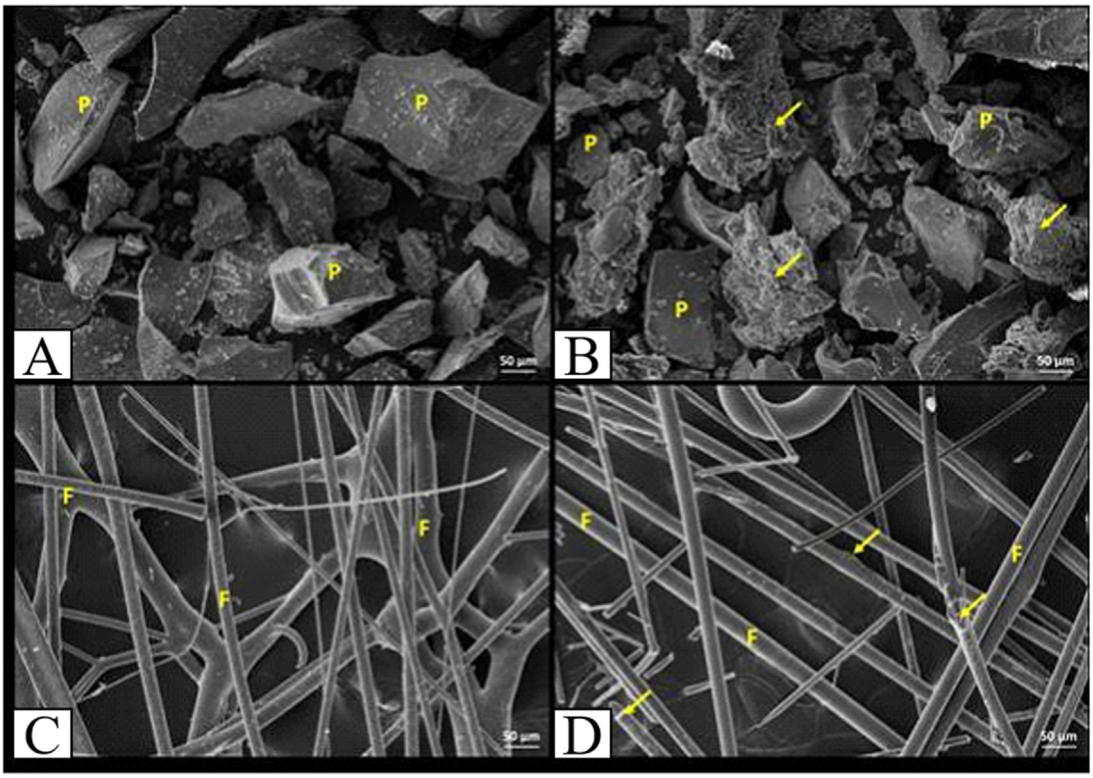

Fig. 1. SEM micrographs of the different materials. (A) BGp; (B) BGp/COL; (C) BGf; (D) BGf/COL. P, BG particles; F, BG fibers; arrows indicate collagen. 500× magnification.

composition showed a rougher surface due to the collagen coating (BGp/COL; Fig. 1B). Additionally, SEM micrographs showed that BG fibers were successfully obtained from the BG precursor (Fig. 1C). These fibers were randomly positioned, presenting different diameters (ranging from 500 nm to 1 mm) (Fig. 1C and D). The fiber surface became more irregular after coating with collagen (BGf/COL; Fig. 1D).

3.1.2. FTIR

Fig. 2A and B present the spectra evaluated by FTIR technique for BG both in powder and fibers form, respectively. The peaks and/or bands have been interpreted in accordance with the data available in the literature. In both spectrograms, the glasses show the characteristic peaks of BG structure (essentially a soda-lime glass modified with P_2O_5) indicated by 1, 6, 7, 8, 10 and 11 in Figs. 2 and 3, where a wide distribution Q^X silica species can be seen observed from Q^0 to Q^4. This distribution is due alkali metals (Na^+ and R^{++}) and phosphate ions accommodation in glass network. The lowest relative intensity of the peaks (indicated by 7 and 8) (Si—O Q^0 and Q^1 respectively), where the oxygens are non-bridging type may indicate that the bioglass in powder form has more cohesive structure that bioglass in the form of fibers. Moreover, the indicative peak of links Na—O (compensator charges in the most disorganized regions in the amorphous structure/number 12) is less apparent in form of

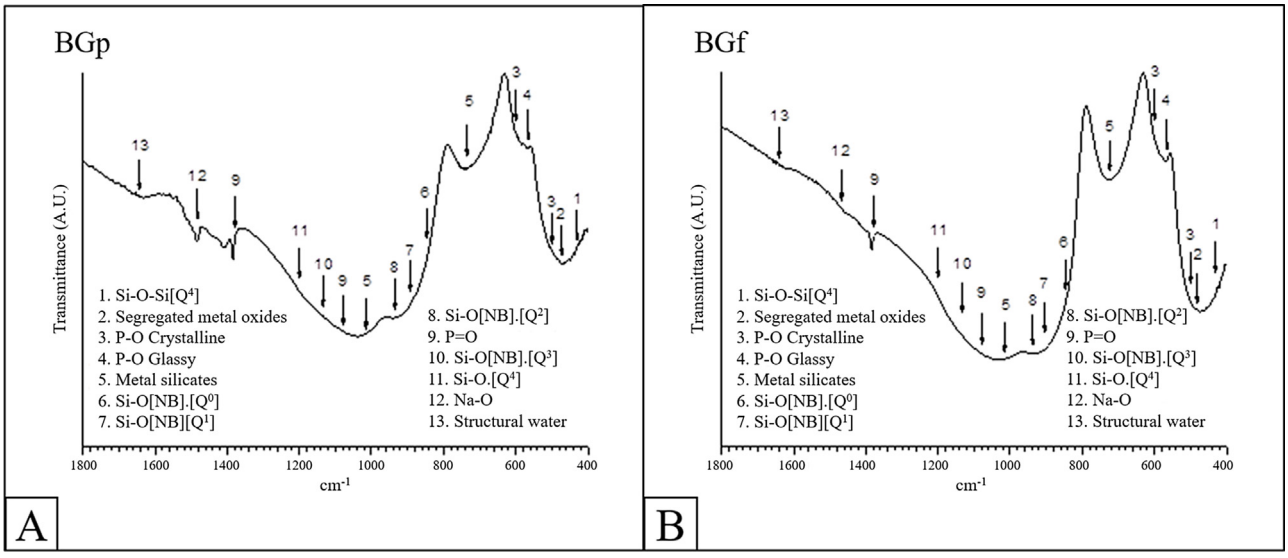

Fig. 2. (A) BGp as obtained FTIR spectra. (B) BGf as obtained FTIR spectra.

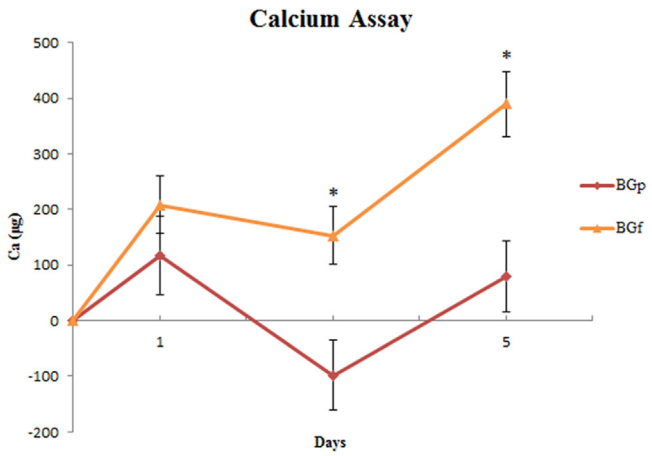

Fig. 3. Calcium assay for BGp and BGf immersed in SBF for up to 5 days. (*) BGf compared to BGp ($p < 0.0063$).

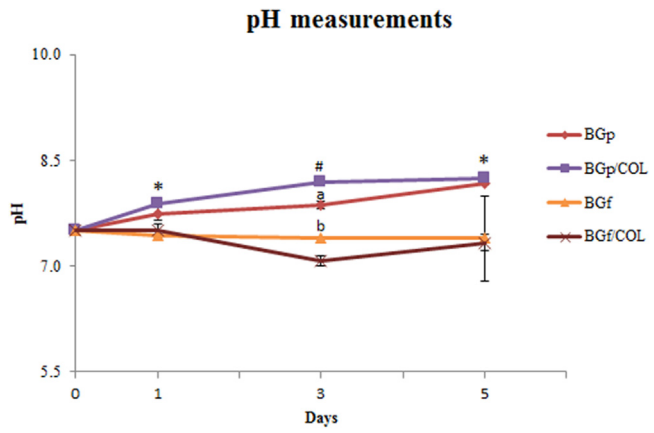

Fig. 4. pH measurements of SBF solution in contact with all compositions for up to 5 days. (*) BGp and BGp/COL compared to the other groups ($p < 0.0005$); (#) BGp/COL compared to all other groups ($p < 0.0008$); (a) BGp compared to BGf and BGf/COL ($p < 0.0002$); (b) BGf compared to BGf/COL ($p < 0.0008$).

fiber BG. Moreover, in both BGs (powder or fibers), a wide distribution of phosphorus cations in the structure is observed (3, 4 and 9).

3.1.3. Calcium assay

The Ca concentration in the SBF was measured quantitatively as a function of soaking time (Fig. 3). Both bioactive materials, BGp and BGf, presented at day 1 an initial Ca uptake with no statistical difference between groups ($p > 0.05$). Three days after incubation, a statistically higher Ca up take for BGf compared to BGp (~55 µg; $p = 0.006$) was observed. Similar behavior was observed five days of immersion, with a higher Ca uptake in BGf (~390 µg) compared to BGp (~80.22 µg; $p = 0.004$).

3.1.4. pH measurements

The evaluation of the pH measurements are indicated in Fig. 4. After 1 day of incubation, the pH values for BGp and BGp/COL were statistically higher compared to BGf and BGf/COL (p values <0.0005). At day 3 of immersion, statistical differences ($p < 0.05$) were observed among all groups (values in descending order: 8.19, 7.87, 7.40 and 7.07 for BGp/COL, BGp, BGf and BGf/COL in that order). At the last experimental period, the pH values were statistically higher for BGp and BGp/COL (~8.2) compared to BGf and BGf/COL (~7.4; $p < 0.0002$).

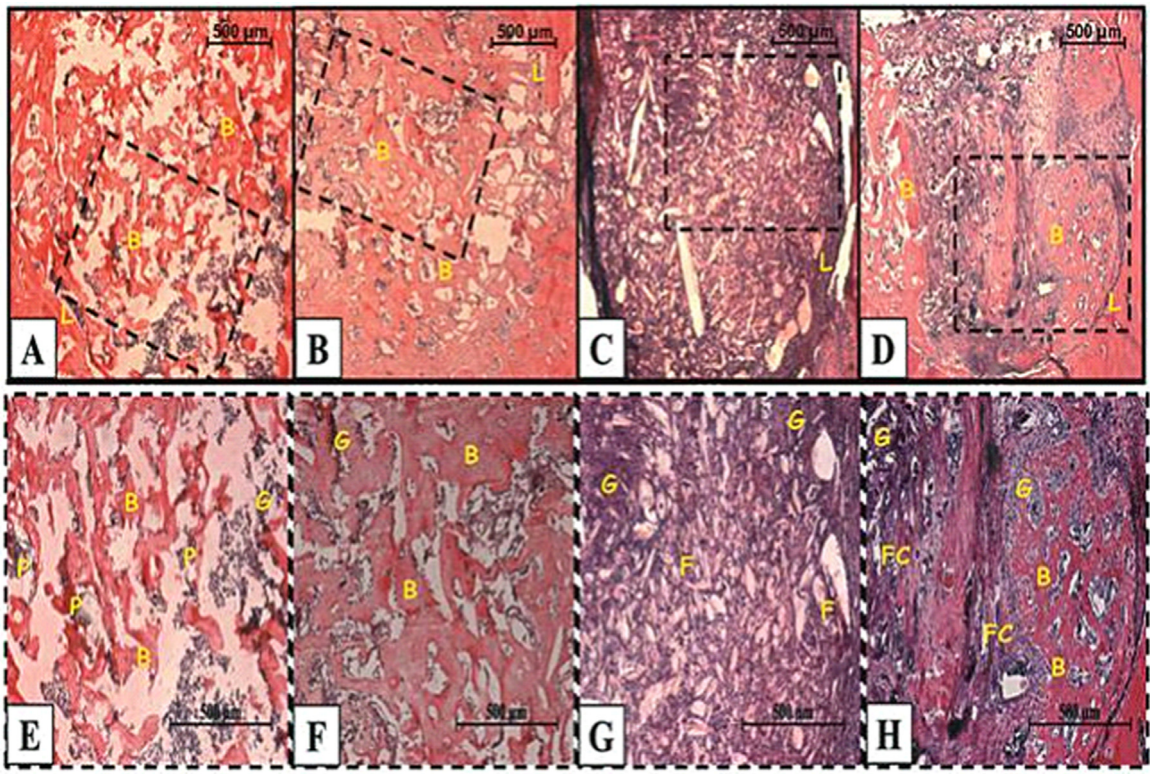

Fig. 5. Histological sections of all groups after 15 days of implantation. (A) BGp, (B) BGp/COL, (C) BGf, (D) BGf/COL. Newly formed bone B, defect line L. Magnification of 2.5×. Dashed box indicates the selected region for analysis at a higher magnification of 20×. (E) BGp, (F) BGp/COL, (G) BGf, (H) BGf/COL. Newly formed bone B, powder P, fibers F, fibers and collagen FC, granulation tissue G. Bar represents 500 µm. Hematoxylin–Eosin staining.

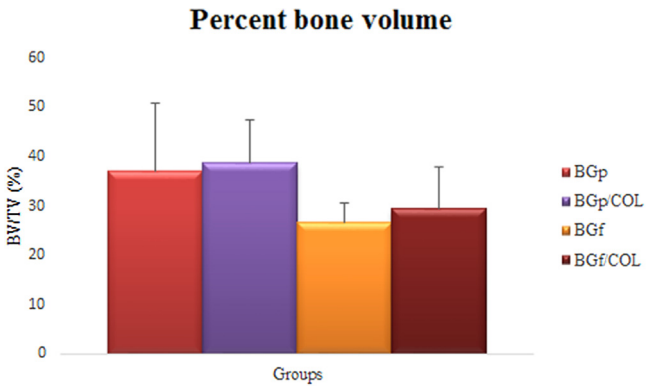

Fig. 6. Percent bone volume – BV/TV (%). Percentage of area within ROI occupied by bone. All data are expressed as Mean (SD). $p < 0.05$.

3.2. In vivo *studies*

3.2.1. *General observation of the experimental animals*

From the 40 animals used in this study, 3 animals were lost due to an anesthesia-induced respiratory depression. The remaining animals recovered uneventfully from the surgical procedure and remained in good health during the entire implantation period. No clinical sign of inflammation or adverse tissue response were observed during the implantation period.

3.2.2. *Histopathological analysis*

The representative histological sections of all experimental groups 2 weeks post-surgery are presented in Fig. 5. The defect line was still observed for all groups and a minor amount of newly formed bone was found in BGf (Fig. 5C) compared to the other groups. Histological findings at a higher magnification (20×) are depicted in Figs. 5E–H for BGp, BGp/COL, BGf and BGf/COL in that order. The histological analysis demonstrated that no inflammatory process was noticed in any specimens of all groups.

For BGp and BGp/COL, similar histological patterns were observed, since for both groups, the bone defect area was filled by newly formed bone, with discrete presence of granulation tissue. Interestingly, the particles of the material were still present for BGp while for BGp/COL, in most cases, the material was almost completely degraded and the defect area was filled by woven bone (Fig. 5E and F).

In regards to BGf, histology assessment revealed that fibers still could be observed in the area of the defect. Moreover, an intense presence of granulation tissue was observed, especially around the biomaterial particles (Fig. 5G). On the other hand, BGf/COL implants presented a more intense degradation accompanied by the formation of immature bone at the periphery of the defect. Additionally, granulation tissue was still observed in the central region of the defect, also filling the spaces previously occupied by the degraded material. Some fibers still could be noticed (Fig. 5H).

3.2.3. *Histomorphometry analysis*

The histomorphometry indicated, after 2 weeks of implantation, that BGf presented a significant decrease in the amount of newly formed bone (approximately 17%) compared to all other groups

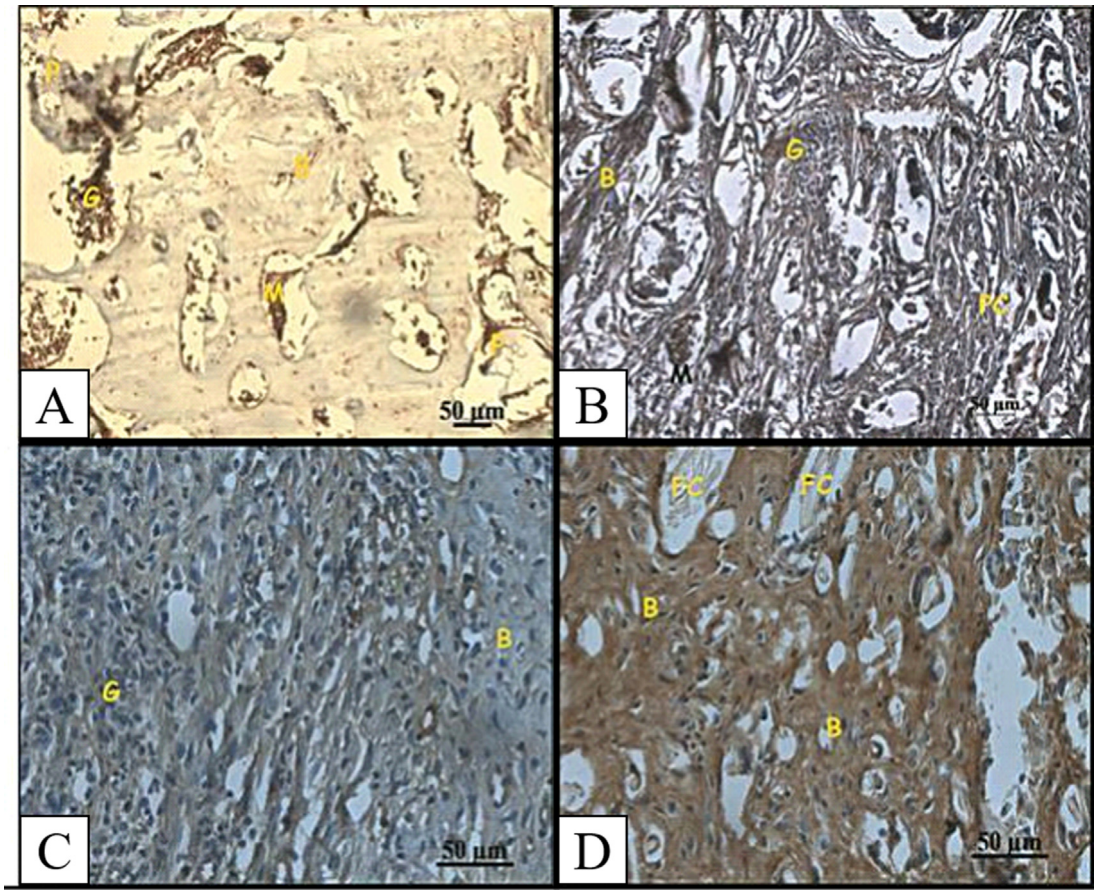

Fig. 7. Immunohistochemistry of RUNX-2. (A) BGp, (B) BGp/COL, (C) BGf, (D) BGf/COL. Newly formed bone B, granulation tissue G, medullar tissue M, powder P, powder and collagen PC, fibers and collagen FC. Bar represents 50 µm. Magnification of 40×.

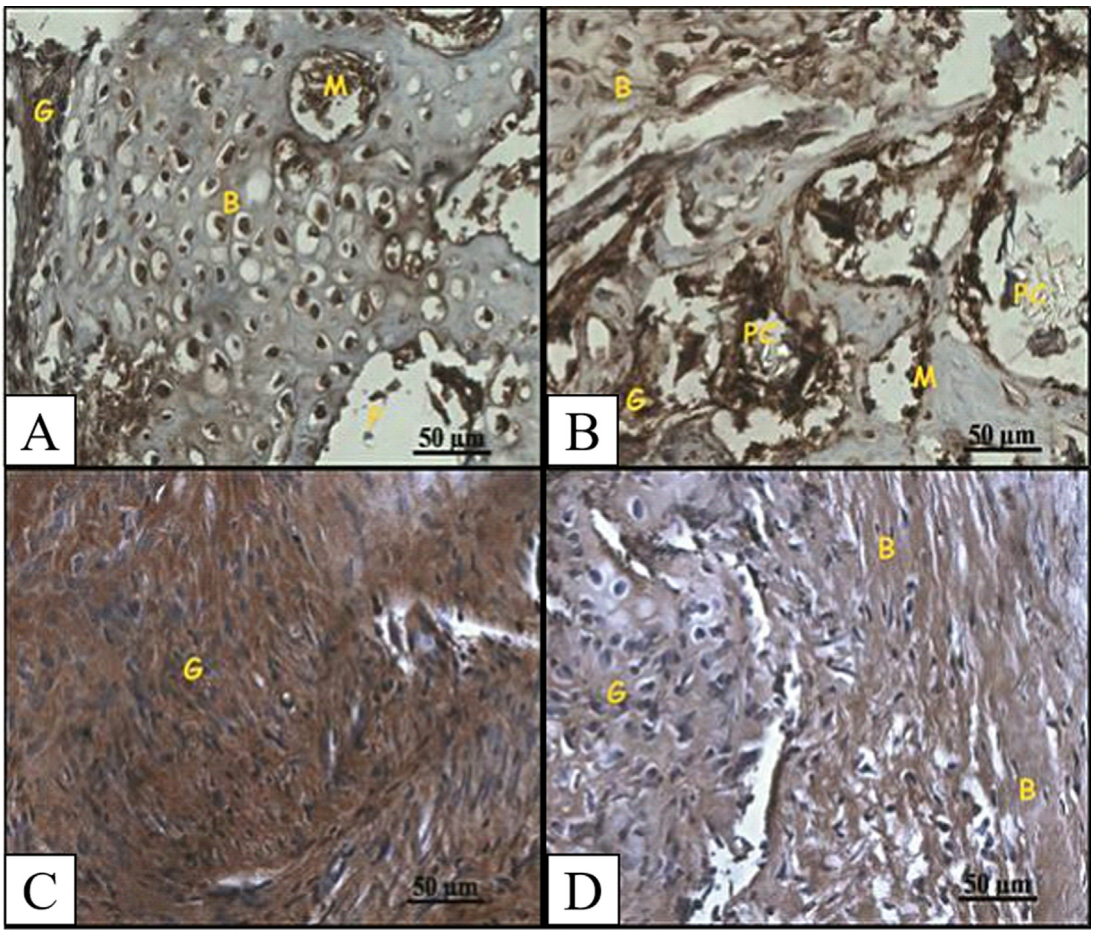

Fig. 8. Immunohistochemistry of RANK-L. (A) BGp, (B) BGp/COL, (C) BGf, (D) BGf/COL. Newly formed bone B, granulation tissue G, medullar tissue M, powder P, powder and collagen PC, fibers and collagen FC. Bar represents 50 µm. Magnification of 40×.

(approximately 38, 54, and 36% for BGp, BGp/COL and BGf/COL respectively; $p < 0.05$). No other difference was observed among groups ($p > 0.05$, Fig. 6).

3.2.4. *Immunohistochemistry analysis*

The immunostaining for RUNX-2 was noticed mainly in the granulation tissue and in the newly formed bone (Fig. 7). For BGp and BGp/COL, RUNX-2 immunoexpression was also noticed in the medullar tissue (Fig. 7A and B). In BGf/COL, RUNX-2 expresssion was detected predominantly in the borders of the defect throughout the neoformed bone (Fig. 7D).

RANK-L immunoexpression was found predominantly in the newly formed bone and granulation tissue (Fig. 8). The medullar tissue was also marked for BGp and BGp/COL (Fig. 8A and B). The granulation tissue and newly formed bone were evidently marked in BGf and BGf/COL respectively (Fig. 8C and D).

4. Discussion

The present study aimed to evaluate and to compare the effect of collagen incorporation into BG powder and fibers, *via* material characterization (morphology, pH evaluation and calcium release of the different materials) and biological evaluation by tibial bone implantation. The hypotheses were that the fibrous material would have a more adequate morphology and the incorporation of collagen into this material would present a more appropriate composition toward to attract bone cell growth, facilitating bone formation. Although presenting different forms, the FTIR analysis indicated that BGp and BGf maintained the characteristic peaks for this class of material. Furthermore the calcium assay showed an increased Ca uptake in the BG fibers. The pH measurements revealed that BGp (with or without collagen) presented higher pH values compared to BGf. In addition, the histological analysis demonstrated no inflammation for all groups at the site of the injury, besides a faster material degradation and higher bone ingrowth for groups with collagen. The immunohistochemistry analysis demonstrated Runx-2 and Rank-L expression for all the groups.

Bone grafts chemically, structurally and mechanically matching natural bone are a promising therapeutic approach being used as bone substitutes [1]. Once bone tissue is composed by organic material (mainly Type 1 collagen) and inorganic substances (most of which hydroxyapatite), synthetic bone grafts should present similar composition [1]. Based on these statements, the composites used in the present study were manufactured in order to mimic bone tissue components, combining a bioactive glass ceramic and collagen [5]. Several studies already demonstrated that BGs have osteoconductive properties and are able of inducing osteogenesis in experimental bone defect models and clinical studies [5,26]. Also, collagen being a natural structural protein and the main component of the extra cellular matrix, is important to attract cells, and support their growth and proliferation [27].

For the FTIR, the peaks and/or bands were interpreted according to the data available in the literature [28–30]. It is important to note that each glass structure is unique, *i.e.*, the amorphous structural arrangement is a result of the thermal history of each glass, even if they have identical chemical composition [7,31]. As each glass was

processed differently (water quenching to glass powder and Hager-Rosengarth [23] process for glass fiber) is natural that between them are observed small differences in the structural arrangement. Such differences may eventually lead to different behaviors in the bioactivity [7,32] of these materials.

The calcium assay showed an increased Ca uptake for BGf comparing to BGp. This event may be explained by the increased cohesion [33] presented by BGf (preserving the surface microstructure), leading to a greater Ca deposition on the material surface [34]. In contrast to that, at day 3, BGp presented a substantially higher Ca release into the medium compared to BGf. It is suggested that the increased surface area presented by BGp generates a higher contact between the material and solution, which may lead to a faster material dissolution and, consequently, faster ion release [35]. Previous studies also indicated that, depending on the material cohesion, distinct formulations containing Biosilicate® (a kind of vitroceramic) have showed different pace of reaction, interfering on the amount of calcium released into the SBF [35].

The pH evaluation for all groups demonstrated that the values reached a maximum of 8.2 and a minimum of 7.1, which are values considered close to the physiological pH. Interestingly, BG samples in powder (with or without collagen) demonstrated a higher pH at all time points analyzed compared to the samples in fibers. It is well known that the release of cations (Si, Na, Ca and P) occurs immediately after the contact of BG with fluids, resulting in an increased pH [36]. Probably, the higher contact surface area of the powder material was responsible by a faster degradation and, consequently, a greater ion release, resulting in an increased pH. Interestingly, the addition of collagen had no effect in the pH measurements for the BG-based materials in both forms.

Furthermore, the histological findings demonstrated that the BG in powder constituted the material with superior biological response compared to the fibers. Interestingly, similar histological results were found between BGp and BGp/COL, although a tendency of higher bone volume for BGp/COL was noted. It may be suggested that the possible accelerated ion release from the powder could be responsible by an enhancement of the biological response [31,37]. This event would provide a more biologically active bone-like apatite layer on the material surface, directing new bone ingrowth into BG-based granular material [7,31].

Additionally, the material in fibers enriched with collagen presented higher bone volume compared to BGf. Collagen is the most abundant protein in the extra celular matrix (ECM), being the major organic component of natural bone. It plays an important role in cell attachment, mechanical support and apatite nucleation [38]. In this context, collagen is also related to the process of bone regeneration and remodeling, promoting cell adhesion and proliferation, and osteogenic differentiation [39,40]. In view of this considerations, it is suggested that the addition of collagen constituted a stimulus for enhancing the biological performance of the fibers. Accordingly, Long et al. [41] demonstrated good biological properties of a scaffolds manufactured with BG and collagen, such as biocompatibility, mechanical stability and adequate porosity, allowing the spreading and proliferation of human bone marrow stromal cells [41].

Concerning the immunohistochemistry, it is noteworthy that RUNX-2 expression was higher in BG when compared to CG on 15 days after implantation. RUNX-2 immunofactor is mainly expressed to central control of the osteoblast phenotype and it is required for the differentiation of mesenchymal progenitors toward osteoblast cell lineage. It is well known that RUNX-2 is fundamental for upregulation of other osteoblastic markers, like osteocalcin, osteopontin and alkaline phosphatase [42], which may have influenced osteoblast cell differentiation and consequently, bone formation and deposition. The *in vivo* findings observed in this study are in agreement with previous studies which have detected higher RUNX-2 immunoexpression in tibial and calvaria defect models filled with Biosilicate® [43,44].

Additionally, the resorption and remodeling of bone tissue by osteoclasts are also necessary for a successful bone healing process. Furthermore, the RANK-L is a key factor for differentiation and activation of osteoclasts [45–47]. Furthermore, the increase of the RANK-L concentration can be related to number of osteogenic cells, once this factor is expressed by osteoblasts [48]. In this context, a higher immunoexpression of RANK-L could be combined with the increase of the osteoblasts and an attempt of degradation the material. Investigations conducted by Pinto et al. [49] verified a more evident immunoexpression of RANK-L around the particles of Biosilicate® glass-ceramic in tibial defects. Similar findings were observed by Kondo et al. [50] who tested b- tricalcium phosphate (b-TCP) using implantation in femoral condyle of rats.

There is a continuous investigation trying to find the more appropriate way for material presentation to be used as bone grafts, which would facilitate vascularization and bone ingrowth. In this context, two different forms of BG, in powder and in fibers, enriched with collagen were tested. Indeed, both forms could stimulate bone repair and, interestingly, the incorporation of collagen improved bone formation only for BG in fibers. The next steps of this work would rely on the obtainment of scaffolds of both BG forms combined with collagen, based on the mineral and organic constitution of the original bone (~70% mineral matrix and ~30% organic matrix) [1], mimicking natural bone. Additionally, it would be of great value to test these materials using critical-size bone defect (CSD) [51], in which bone consolidation does not happen spontaneously. Following this line, further investigations are necessary to validate these combinations as safe and efficient materials for biomedical applications.

5. Conclusions

Treatment of BGp/COL showed better results mainly by its shape and composition. This combination seems to be a promising alternative for bone tissue engineering cause an enhanced release of Ca and accelerated bone process repair by advanced osteoconductive properties. More efforts are needed to further present other mechanism that this biomaterial is capable of interact/activate.

Conflicts of interest

The authors declare that they have no competing interests.

Acknowledgments

We thank the Brazilian funding agencies FAPESP and CAPES for the financial support of this research.

References

[1] Y.S. Pek, S. Gao, M.S. Arshad, K.J. Leck, J.Y. Ying, Porous collagen-apatite nanocomposite foams as bone regeneration scaffolds, Biomaterials 29 (2008) 4300–4305.
[2] V.V. Välimäki, H.T. Aro, Molecular basis for the action of bioactive glasses as bone graft, Scand. J. Surg. 95 (2006) 95–102.
[3] L.L. Hench, J.M. Polak, Third-generation biomedical materials, Science 295 (2002) 1014–1017.
[4] I.D. Xynos, A.J. Edgar, L.D.K. Buttery, L.L. Hench, J.M. Polak, Ionic Products of Bioactive Glass Dissolution Increase Proliferation of Human Osteoblasts and Induce Insulin-like Growth Factor II mRNA Expression and Protein Synthesis, Biochem. Biophys. Res. Commun. 276 (2000) 461–465.
[5] L.L. Hench, I.D. Xynos, J.M. Polak, Bioactive glasses for in situ tissue regeneration, J. Biomater. Sci. Polym. Ed. 15 (2004) 543–562.
[6] L.L. Hench, Glass and genes: the 2001 W.E.S. Turner Memorial Lecture, Glass Technol. 44 (2003) 1–10.
[7] L.L. Hench, The story of bioglass, J. Mater. Sci. Mater. Med. 17 (2006) 967–978.
[8] A.C. Renno, M.R. Nejadnik, F.C. van de Watering, M.C. Crovace, E.D. Zanotto, J.P. Hoefnagels, J.G. Wolke, J.A. Jansen, J.J. van den Beucken, Incorporation of

bioactive glass in calcium phosphate cement: material characterization and in vitro degradation, J. Biomed. Mater. Res. Part A 101 (2013) 2365–2373.
[9] K. Rezwan, Q.Z. Chen, J.J. Blaker, A.R. Boccaccini, Biodegradable and bioactive porous polymer/inorganic composite scaffolds for bone tissue engineering, Biomaterials 27 (2006) 3413–3431.
[10] S.S. Liao, F.Z. Cui, W. Zhang, Q.L. Feng, Hierarchically biomimetic bone scaffold materials: nano-HA/collagen/PLA composite, J. Biomed. Mater. Res. Part B Appl. Biomater. 69 (2004) 158–165.
[11] Y.S. Pek, M. Spector, I.V. Yannas, L.J. Gibson, Degradation of a collagen-chondroitin-6-sulfate matrix by collagenase and by chondroitinase, Biomaterials 25 (2004) 473–482.
[12] C. Xu, P. Su, X. Chen, Y. Meng, W. Yu, A.P. Xiang, Y. Wang, Biocompatibility and osteogenesis of biomimetic Bioglass-Collagen-Phosphatidylserine composite scaffolds for bone tissue engineering, Biomaterials 32 (2011) 1051–1058.
[13] B. Marelli, C.E. Ghezzi, D. Mohn, W.J. Stark, J.E. Barralet, A.R. Boccaccini, S.N. Nazhat, Accelerated mineralization of dense collagen-nano bioactive glass hybrid gels increases scaffold stiffness and regulates osteoblastic function, Biomaterials 32 (2011) 8915–8926.
[14] M. Spector, Biomaterials-based tissue engineering and regenerative medicine solutions to musculoskeletal problems, Swiss Med. Wkly. 136 (2006) 293–301.
[15] M. Mastrogiacomo, S. Scaglione, R. Martinetti, L. Dolcini, F. Beltrame, R. Cancedda, R. Quarto, Role of scaffold internal structure on in vivo bone formation in macroporous calcium phosphate bioceramics, Biomaterials 27 (2006) 3230–3237.
[16] C. Wu, Y. Zhu, J. Chang, Y. Zhang, Y. Xiao, Bioactive inorganic-materials/alginate composite microspheres with controllable drug-delivery ability, J. Biomed. Mater. Res. Part B Appl. Biomater. 94 (2010) 32–43.
[17] A.R. Boccaccini, V. Maquet, Bioresorbable and bioactive polymer/bioglass® composites with tailored pore structure for tissue engineering applications, Compos. Sci. Technol. 63 (2003) 2417–2429.
[18] P.R. Gabbai-Armelin, M.T. Souza, H.W. Kido, C.R. Tim, P.S. Bossini, K.R. Fernandes, A.M. Magri, N.A. Parizotto, K.P. Fernandes, R.A. Mesquista-Ferrari, D.A. Ribeiro, E.D. Zanotto, O. Peitl-Filho, A.C. Renno, Characterization and biocompatibility of a fibrous glassy scaffold, J. Tissue Eng. Regen. Med. 11 (4) (2015) 1141–1151, http://dx.doi.org/10.1002/term.2017.
[19] E.I. Pascu, J. Stokes, G.B. McGuinness, Electrospun composites of PHBV, silk fibroin and nano-hydroxyapatite for bone tissue engineering, Mater. Sci. Eng. C Mater. Biol. Appl. 33 (2013) 4905–4916.
[20] P.R. Gabbai-Armelin, M.T. Souza, H.W. Kido, C.R. Tim, P.S. Bossini, A.M. Magri, K.R. Fernandes, F.A. Pastor, E.D. Zanotto, N.A. Parizotto, O. Peitl, A.C. Renno, Effect of a new bioactive fibrous glassy scaffold on bone repair, J. Mater. Sci. Mater. Med. 26 (2015) 5516.
[21] F. Braga, A.C. da Silva, S. Allegrini Jr, C. Ottoni, Calcium phosphate graft substitute: when the impact of innovation is in the form rather than content, in: E (Ed.), 26th Annual Conference of the European Society of Biomaterials, Liverpool, 2014.
[22] R. Friedrich, H. Fritz, Apparatus and Method for Production of Fibers from Glass, Slag, and the Like Meltable Materials, Google Patents, (1941).
[23] J.M.F. Navarro, El Vidrio, Consejo Superior de Invest, Científicas – Fundación Centro Nacional del Vidrio, Madrid, 2003.
[24] T. Kokubo, H. Takadama, How useful is SBF in predicting in vivo bone bioactivity? Biomaterials 27 (2006) 2907–2915.
[25] R.E. Mooren, E.J. Hendriks, J.J. van den Beucken, M.A. Merkx, G.J. Meijer, J.A. Jansen, P.J. Stoelinga, The effect of platelet-rich plasma in vitro on primary cells: rat osteoblast-like cells and human endothelial cells, Tissue Eng. Part A 16 (2010) 3159–3172.
[26] R.N. Granito, D.A. Ribeiro, A.C. Renno, C. Ravagnani, P.S. Bossini, O. Peitl-Filho, E.D. Zanotto, N.A. Parizotto, J. Oishi, Effects of biosilicate and bioglass 45S5 on tibial bone consolidation on rats: a biomechanical and a histological study, J. Mater. Sci. Mater. Med. 20 (2009) 2521–2526.
[27] N. Zhao, D. Zhu, Collagen self-assembly on orthopedic magnesium biomaterials surface and subsequent bone cell attachment, PLoS One 9 (2014) e110420.
[28] S.A. MacDonald, C.R. Schardt, D.J. Masiello, J.H. Simmons, Dispersion analysis of FTIR reaction measurements in silicate glasses, J. Non-Cryst. Solids (2000) 72–82.
[29] H. Arizpe-Chavez, Ma E. Zayas, F.J. Espinola-Beltrán, C. Díaz, L.L. Díaz-Flores, J.M. Yáñez-Limón, J. Gonzáles-Hernández, Spectroscopic studies on Na2O–SiO2 glasses with different Ag concentration using silica obtained from wastes of a geothermal plant, J. Non-Cryst. Solids 324 (2003) 67–72.
[30] O. Peitl, E.D. Zanotto, L.L. Hench, Highly bioactive P2O5–Na2O–CaO–SiO2 glass-ceramics, J. Non-Cryst. Solids 292 (2001) 115–126.
[31] L.L. Hench, Introduction to Bioceramics, 2nd ed., Imperial College Press, London, 2013, pp. 620, ISBN: 978-1-908977-15-1.
[32] L.L. Hench, T. Kokubo, Properties of bioactive glasses and glass-ceramics, in: J. Black, G. Hastings (Eds.), Handbook of Biomaterial Properties, Springer, US, 1998, pp. 355–363.
[33] D.W. Jackson, T.M. Simon, Tissue engineering principles in orthopaedic surgery, Clin. Orthop. Relat. Res. (1999) S31–S45.
[34] N. Davison, H. Yuan, J.D. de Bruijn, F. Barrere-de Groot, In vivo performance of microstructured calcium phosphate formulated in novel water-free carriers, Acta Biomater. 8 (2012) 2759–2769.
[35] P.R. Gabbai-Armelin, D.A. Cardoso, E.D. Zanotto, O. Peitl, S.C.G. Leeuwenburgh, J.A. Jansen, A.C.M. Renno, J.J.J.P. van den Beucken, Injectable composites based on biosilicate[registered sign] and alginate: handling and in vitro characterization, RSC Adv. 4 (2014) 45778–45785.
[36] V.V. Valimaki, N. Moritz, J.J. Yrjans, M. Dalstra, H.T. Aro, Peripheral quantitative computed tomography in evaluation of bioactive glass incorporation with bone, Biomaterials 26 (2005) 6693–6703.
[37] D. Deborah, L. Wei, A.R. Judith, W.S. Dirk, C.C. Murilo, M.R. Ana Candida, D.Z. Edgar, R.B. Aldo, Biosilicate® –gelatine bone scaffolds by the foam replica technique: development and characterization, Sci. Technol. Adv. Mater. 14 (2013) 045008.
[38] E. Saino, S. Grandi, E. Quartarone, V. Maliardi, D. Galli, N. Bloise, L. Fassina, M.G. De Angelis, P. Mustarelli, M. Imbriani, L. Visai, In vitro calcified matrix deposition by human osteoblasts onto a zinc-containing bioactive glass, Eur. Cells Mater. 21 (2011) 59–72, discussion 72.
[39] M. Geiger, R.H. Li, W. Friess, Collagen sponges for bone regeneration with rhBMP-2, Adv. Drug Deliv. Rev. 55 (2003) 1613–1629.
[40] M.P. Bostrom, D.A. Seigerman, The clinical use of allografts, demineralized bone matrices, synthetic bone graft substitutes and osteoinductive growth factors: a survey study, HSS J. Musculoskelet. J. Hosp. Spec. Surg. 1 (2005) 9–18.
[41] T. Long, J. Yang, S.-S. Shi, Y.-P. Guo, Q.-F. Ke, Z.-A. Zhu, Fabrication of three-dimensional porous scaffold based on collagen fiber and bioglass for bone tissue engineering, J. Biomed. Mater. Res. Part B Appl. Biomater. 103 (7) (2014) 1455–1464, http://dx.doi.org/10.1002/jbm.b.33328.
[42] F. Afzal, J. Polak, L. Buttery, Endothelial nitric oxide synthase in the control of osteoblastic mineralizing activity and bone integrity, J. Pathol. 202 (2004) 503–510.
[43] P.S. Bossini, A.C. Renno, D.A. Ribeiro, R. Fangel, O. Peitl, E.D. Zanotto, N.A. Parizotto, Biosilicate(R) and low-level laser therapy improve bone repair in osteoporotic rats, J. Tissue Eng. Regen. Med. 5 (2011) 229–237.
[44] M.A. Matsumoto, G. Caviquioli, C.C. Biguetti, A. Holgado Lde, P.P. Saraiva, A.C. Renno, R.Y. Kawakami, A novel bioactive vitroceramic presents similar biological responses as autogenous bone grafts, J. Mater. Sci. Mater. Med. 23 (2012) 1447–1456.
[45] V. Lemaire, F.L. Tobin, L.D. Greller, C.R. Cho, L.J. Suva, Modeling the interactions between osteoblast and osteoclast activities in bone remodeling, J. Theor. Biol. 229 (2004) 293–309.
[46] A.E. Kearns, S. Khosla, P.J. Kostenuik, Receptor activator of nuclear factor kappaB ligand and osteoprotegerin regulation of bone remodeling in health and disease, Endocr. Rev. 29 (2008) 155–192.
[47] A.P. Anandarajah, E.M. Schwarz, Bone loss in the spondyloarthropathies: role of osteoclast, RANKL, RANK and OPG in the spondyloarthropathies, Adv. Exp. Med. Biol. 649 (2009) 85–99.
[48] S. Reppe, H. Datta, K.M. Gautvik, The influence of DNA methylation on bone cells, Current genomics 16 (2015) 384–392.
[49] K.N. Pinto, C.R. Tim, M.C. Crovace, M.A. Matsumoto, N.A. Parizotto, E.D. Zanotto, O. Peitl, A.C. Renno, Effects of biosilicate((R)) scaffolds and low-level laser therapy on the process of bone healing, Photomed. Laser Surg. 31 (2013) 252–260.
[50] N. Kondo, A. Ogose, K. Tokunaga, T. Ito, K. Arai, N. Kudo, H. Inoue, H. Irie, N. Endo, Bone formation and resorption of highly purified beta-tricalcium phosphate in the rat femoral condyle, Biomaterials 26 (2005) 5600–5608.
[51] C. Bosch, B. Melsen, K. Vargervik, Importance of the critical-size bone defect in testing bone-regenerating materials, J. Craniofac. Surg. 9 (1998) 310–316.